Journal of Applied Polymer Science

Biobased Hyperbranched Shape-Memory Polyurethanes: Effect of Different Vegetable Oils

Hemjyoti Kalita, Niranjan Karak
Advanced Polymer and Nanomaterial Laboratory, Department of Chemical Sciences, Tezpur University, Tezpur 784028, Assam, India
Correspondence to: N. Karak (E-mail: karakniranjan@yahoo.com)

ABSTRACT: Hyperbranched polyurethanes were synthesized from poly(ε-caprolactone) diol as a macroglycol, butanediol as a chain extender, a monoglyceride of a vegetable oil (*Mesua ferrea*, castor, and sunflower oils separately) as a biobased chain extender, triethanolamine as a multifunctional moiety, and toluene diisocyanate by a prepolymerization technique with the $A_2 + B_3$ approach. The structure of the synthesized hyperbranched polyurethanes was characterized by ^{1}H-NMR and X-ray diffraction studies. *M. ferrea* L. seed-oil-based polyurethane showed the highest thermal stability, whereas the castor-oil-based one showed the lowest. However, the castor-oil-based polyurethane exhibited the highest tensile strength compared to the other vegetable-oil-based polyurethanes. All of the vegetable-oil-based polyurethanes showed good shape fixity, although the castor-oil-based polyurethane showed the highest shape recovery. Thus, the characteristics of the vegetable oil had a prominent role in the control of the ultimate properties, including the shape-memory behaviors, of the hyperbranched polyurethanes. © 2013 Wiley Periodicals, Inc. J. Appl. Polym. Sci. **2014**, *131*, 39579.

KEYWORDS: composites; elastomers; flame retardance

Received 18 December 2012; accepted 23 May 2013
DOI: 10.1002/app.39579

INTRODUCTION

Nature shows examples of stimuli-responsive phenomenon. For example, the leaves of *Mimosa pudica* fold inward rapidly when they are touched, sunflowers bend toward the sun, and chameleons change color according to the environmental situation.[1] Thus, to mimic nature, enormous efforts have been made to design stimuli-responsive polymers, particularly segmented polyurethanes, which have potential applications in the fields of sensors, microactuators, intelligent biomedical devices, implant materials, self-deployable structures, smart textiles, sporting goods, and so on.[2–7] Shape-memory polyurethanes are not only stimuli-responsive smart polymeric materials, which can respond to a particular external stimuli such as temperature, light, solvent, magnetic field, and electric field by changing their shape, but also possess other desired properties.[3,8,9] The net points, which are the chemically or physically crosslinked network structures of segmented polyurethanes, determine the permanent shape of the polymer network, whereas a switching segment acts as a mobile phase.[10–12] Shapes are driven by the specific transition temperature (T_{trans}), which is either near the glass-transition temperature (T_g) or close to the melting temperature (T_m). However, T_m is generally considered because the melting transition is sharper than T_g.[13,14] Thus, the synthesis of elastic polyurethanes with different structures and properties is an apt choice in recent times.

Furthermore, the realization of finite petroleum resources, growing environmental concerns, and waste disposal problems encourage the utilization of bioresources such as vegetable oils as raw materials for the preparation of polyurethanes.[15–18] This due to the fact that such oils have numerous advantages, including easy availability, relatively low cost, versatility in structure and properties, inherent biodegradability, and environmentally friendliness.[19] Again, the hydroxylation of vegetable oils is one good approach for obtaining the required polyols to be used in polyurethane synthesis. In this investigation, different vegetable oils were modified through transesterification to obtain the desired diols. The properties of vegetable-oil-based polyurethanes depend on the characteristics, that is, the physical and chemical structures, which include the number of hydroxyl groups in the polyols, degree of unsaturation, length of the fatty acid chains, and position of hydroxyl groups in the fatty acid chain.[20,21] Thus, in this study, monoglycerides (MGs) of three vegetable oils with different structures and compositions were used to obtain shape-memory polyurethanes with unique structural architectures.

Among the different polymeric architectures, hyperbranched polyurethanes are winning much attention from materials scientists and technologists because of their highly functionalized, nonentangled structure and easy synthesis.[22] They offer many advantage, including a lower melt and solution viscosity, higher

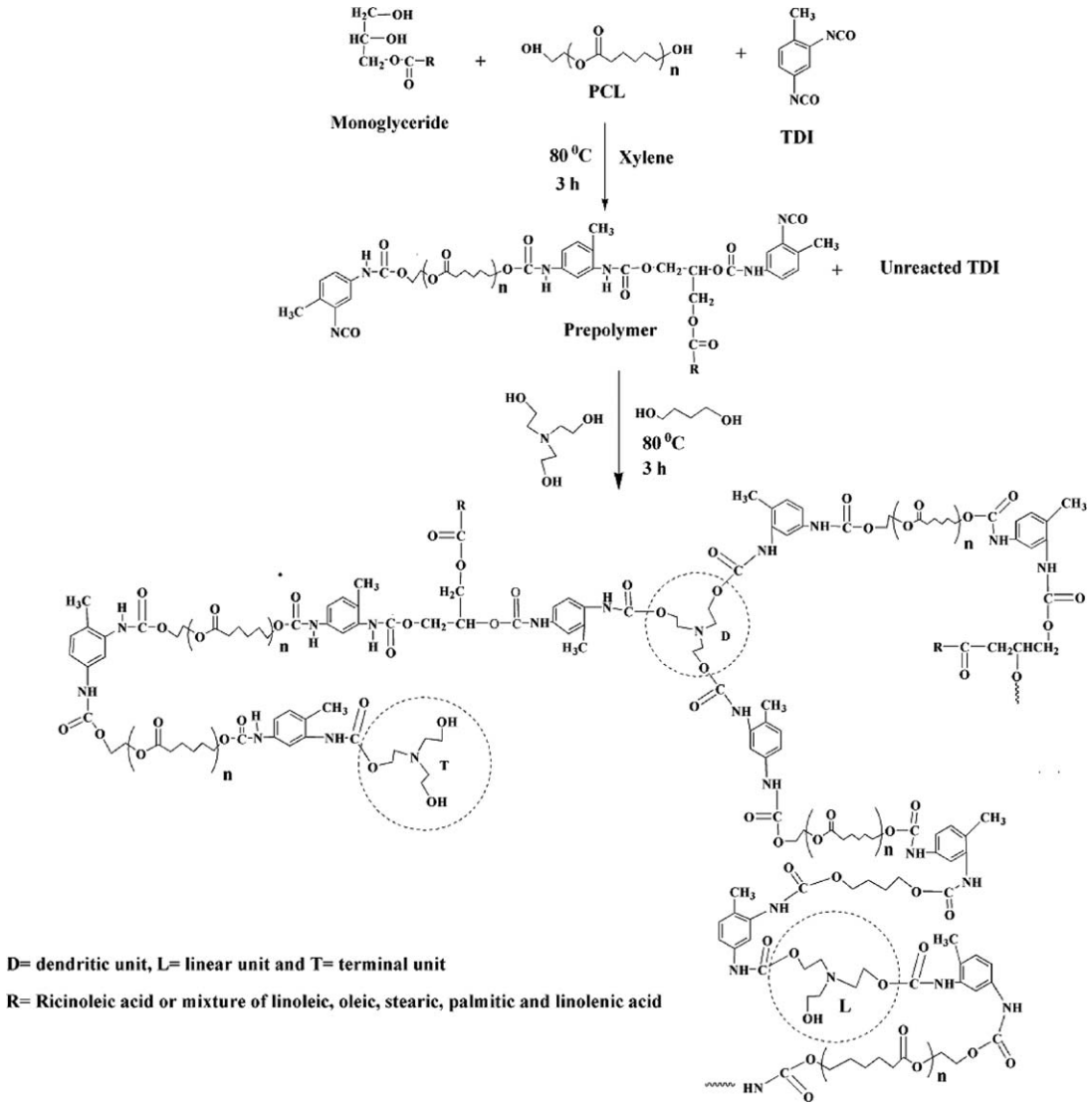

Scheme 1. Synthesis of the vegetable-oil-based hyperbranched polyurethanes.

solubility, and higher reactivity than their linear analogs. However, in general, they suffer from brittleness. This problem was addressed in this study through the incorporation of a long, flexible macroglycol, polycaprolactone diol, and the presence of a long, flexible hydrocarbon chain of the vegetable oils. Therefore, hyperbranched polyurethanes with different vegetable oils and a flexible macroglycol were synthesized as shape-memory polymers.

In this study, hyperbranched polyurethanes with long segments, therefore, were synthesized with MGs of different vegetable oils (*Mesua ferrea,* castor, and sunflower oils) to investigate the effects of the structure and composition of vegetable oils on various properties, including the shape-memory behavior. Polyurethane without vegetable oil was synthesized for comparison purposes.

EXPERIMENTAL

Materials

M. ferrea L. seeds were collected from Darang, Assam, India, and the oil was isolated by a solvent soaking method and purified by an alkali refining technique. Sunflower oil (Sigma, Germany), castor oil (Aldrich Chemical, Castle Hill, Australia), glycerol (Merck, India), poly(ε-caprolactone) diol (PCL; Solvay Co., Japan, number-average molecular weight = 3000 g/mol), 1,4-butanediol (Merck, Germany), and triethanolamine (Merck, India) were used after they were dried in a vacuum oven at 60°C for 12 h. Calcium oxide (S. D. Fine Chemical, Ltd., Mumbai) and toluene diisocyanate (80% of 2, 4, and 20% 2,6 isomers, toluene diisocyanate (TDI), Sigma Aldrich, Germany) were used as received. Xylene (Merck, India) was vacuum-distilled and kept in 4A-type molecular sieves before use.

Preparation of the MGs of the Oils

The MGs of the oils were prepared by a glycerolysis process, as reported earlier.[23] Briefly, a 250-mL, three-necked, round-bottom flask equipped with a nitrogen inlet tube, a thermometer, a heating mantle, and a mechanical stirrer was used for the preparation of the MGs of the vegetable oil. The required amounts of oil (0.023 mol) and glycerol (0.046 mol) were placed in this flask with constant stirring. An amount of 0.05%

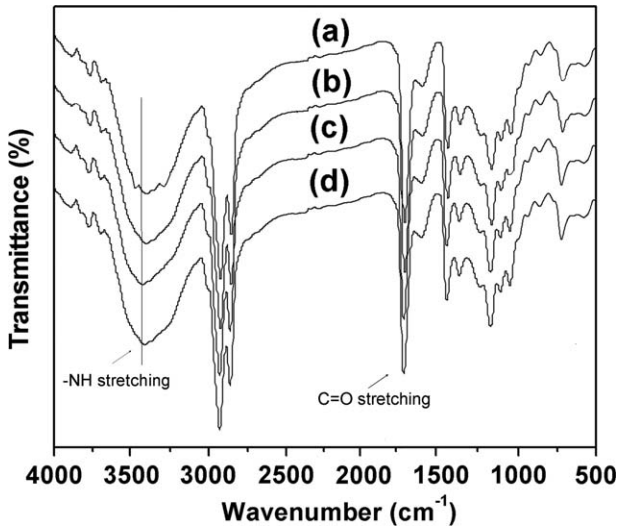

Figure 1. FTIR spectra for (a) CHBPU, (b) MHBPU, (c) SHBPU, and (d) HBPU.

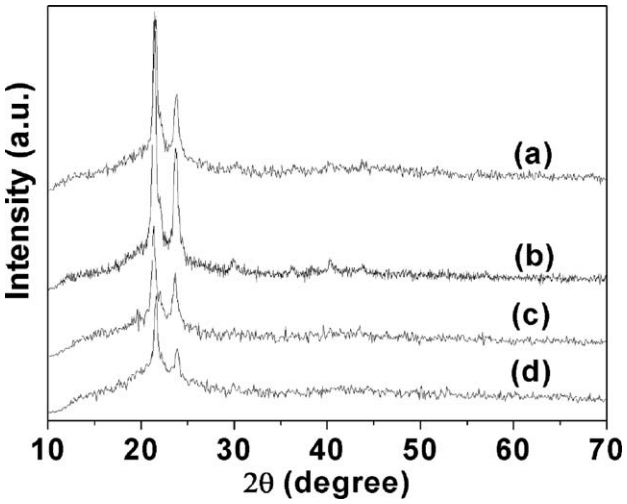

Figure 2. X-ray diffractograms for (a) CHBPU, (b) MHBPU, (c) SHBPU, and (d) HBPU.

(with respect to the oil) CaO was added to the reaction mixture, and then, the temperature was gradually increased up to 220°C. Then the mixture was stirred for 2 h. The formation of the MGs was confirmed by their solubility in methanol (MG/methanol = 1:3 v/v) at room temperature.

Synthesis of the Hyperbranched Polyurethanes

The hyperbranched polyurethanes were synthesized by a two-step, one-pot $A_2 + B_3$ approach (Scheme 1). A 250-mL, three-necked round-bottom flask equipped with a mechanical stirrer, nitrogen inlet tube, and a thermometer was placed in an oil bath for this polymerization reaction. The MGs of *M. ferrea* L. seed oil (3.78 mol) and PCL (2.8 mol) were placed in the reaction flask with 30 mL of xylene with constant stirring. TDI (14.76 mol) was slowly injected into the previous reaction mixture at room temperature. The reaction mixture was allowed to react for 3 h at 80 ± 5°C to obtain the prepolymer. The reaction mixture was then allowed to cool to room temperature, and then, 1,4-butanediol (2 mol) and triethanolamine (4.12 mol) were added drop by drop to the prepolymer (NCO/OH ratio = 1.0). The temperature of the reaction mixture was again raised to 80 ± 5°C and stirred continuously for about another 3 h. After the completion of the reaction, a part of the viscous product was precipitated in water and then dried in a vacuum oven at 60°C for 24 h for the NMR analysis. The remaining part was solution cast on different substrates for other testing. The same procedure was followed for the synthesis of other vegetable-oil-based polyurethanes (the content of MGs of the vegetable oil was 10 wt % in all of the cases) and without oil-based polyurethane. The synthesized hyperbranched polyurethanes were coded CHBPU, MHBPU, SHBPU, and HBPU for castor, *M. ferrea*, sunflower, and no oil-based polyurethanes, respectively.

Measurements

The infrared spectra of the hyperbranched polyurethane were recorded by an Impact 410 Nicolet Fourier transform infrared (FTIR) spectrophotometer (Madison, WI) with KBr pellets. The ^{1}H-NMR spectrum of the polymer was recorded by a 400-MHz NMR spectrometer (JEOL, Japan) with hexadeuterated dimethyl sulfoxide as the solvent and TMS as an internal standard. The X-ray diffraction (XRD) study was carried out at room temperature (ca. 25°C) by a Rigaku X-ray diffractometer (Miniflex, United Kingdom) over a range of $2\theta = 10$–70°. The thermal analysis was done by a Shimadzu thermal analyzer (TG50, Japan) with a nitrogen flow rate of 30 mL/min at a heating rate of 10°C/min. The differential scanning calorimetry (DSC) study was done by a DSC 60 instrument (Shimadzu) at a 3°C/min heating rate under a nitrogen flow rate of 30 mL/min from −30 to 150°C. The tensile strength and elongation at break were measured with the help of a universal testing machine (Zwick Z010, Germany) with a 10 × 10^3-N load cell and a crosshead speed of 0.05 m/min with sample dimensions of 0.1 × 0.01 × 0.00035 m^3. The scratch resistance of the dry film was measured with a scratch hardness tester (model number 705, Sheen Instruments, Ltd., United Kingdom) with a stylus accessory and a travel speed of 0.03–0.04 m/s. The impact

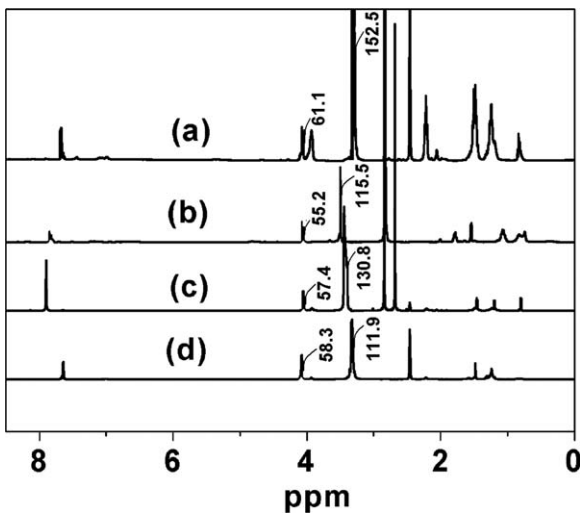

Figure 3. ^{1}H-NMR spectra for (a) CHBPU, (b) SHBPU, (c) MHBPU, and (d) HBPU.

Table I. Structures and Composition of Vegetable Oils

Fatty acid	Structure	*M. ferrea* L. seed oil	Sunflower oil	Castor oil
Palmitic acid (%)	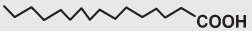	15.9	5.2	—
Stearic acid (%)	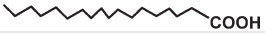	9.5	2.7	—
Oleic acid (%)		52.3	37.2	—
Linoleic acid (%)		22.3	53.8	—
Linolenic acid (%)	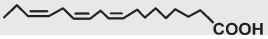	—	1.0	—
Ricinoleic acid (%)		—	—	95

resistance was measured by an impact tester (S. C. Dey & Co., India, 1.0 m was the maximum height) with the standard ASTM D 1037 falling weight method. A weight of 0.85 kg was allowed to fall on the mild steel plate coated film from minimum to maximum height up to which the film was not damaged. The maximum height was taken as the impact resistance.

Shape-Memory Behavior Study

The shape-memory properties of the hyperbranched polyurethanes were determined through a series of thermocyclic tensile experiments by the help of a universal testing machine with a thermal cabinet attachment from Jinan (Republic of China) with a 500-N load cell. At first, the films were cut into rectangular strips with dimensions of 0.04 × 0.005 × 0.0006 m^3 and heated at 60°C ($T_m + 20$°C) for 5 min. Then they were stretched to twice of their original length (L_0) with a stretching rate of 0.02 m/min, and the stretched length was denoted as L_1. Immediately, the stretched samples were frozen at 0–5°C ($T_m - 40$°C) for 5 min to fix the temporary shape, and the length was measured as L_2 after the removal of the load. Subsequently, the samples were reheated at the same temperature (60°C) for the same period of time for shape recovery, and the length obtained was denoted as L_3. The same procedure was followed for the repeated cycles of testing. The shape recovery and shape fixity were two shape-memory parameters calculated from the following equations:

$$\text{Shape recovery}\,(\%) = [(L_1 - L_3)/L_0] \times 100 \quad (1)$$

$$\text{Shape fixity}\,(\%) = [(L_2 - L_0)/L_0] \times 100 \quad (2)$$

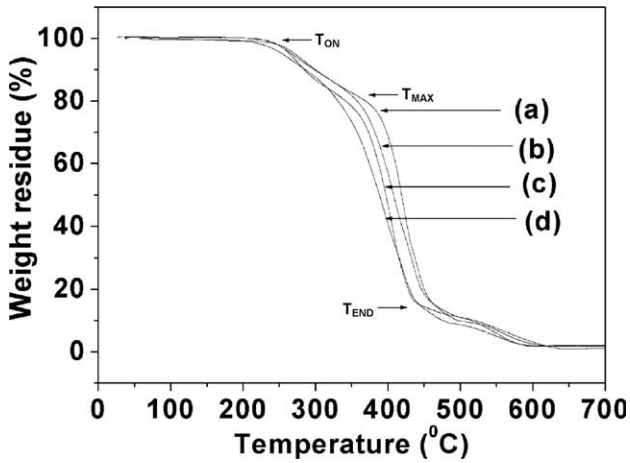

Figure 4. Thermogravimetric analysis thermograms for (a) MHBPU, (b) SHBPU, (c) HBPU, and (d) CHBPU.

RESULTS AND DISCUSSION

Infrared Spectroscopic Study

FTIR spectra of all of the synthesized hyperbranched polyurethanes are shown in Figure 1. The bands appeared at 3406–3430 cm^{-1} for the hydrogen-bonded —NH stretching vibrations, 1720–1725 cm^{-1} for the —C═O stretching vibrations, and 1061 cm^{-1} for the C—O—C stretching vibrations; these are the three characteristic bands of the urethane group. Polyurethane contains a proton donor group (—NH) and a proton acceptor group (>C═O). The —NH groups of the urethane linkages in polyurethane were hydrogen-bonded with —C═O of the urethane linkages and ether oxygen of the soft segments. The bands appearing for the hydrogen-bonded —NH stretching vibrations at 3364 cm^{-1} of HBPU were shifted to 3351, 3359, and 3365 cm^{-1} for the CHBPU, MHBPU, and SHBPU, respectively. Therefore, the —NH stretching frequency shifted to a lower frequency.[24,25] The band appearing at 2926 cm^{-1} was assigned to the —CH stretching of $—CH_2$ and $—CH_3$. The bands at 870 and 730 cm^{-1} were due to the substituted aromatic ring of TDI. The disappearance of the band at 2250–2270 cm^{-1} indicated that there was no residual —NCO group present in the hyperbranched polymer structure, and the reaction was assumed to be completed. All of the previous bands confirmed the formation of urethane groups in the synthesized hyperbranched polyurethanes.

XRD Study

Figure 2 shows X-ray diffractograms of all of the hyperbranched polyurethanes. XRD analysis confirmed the presence of crystallinity of the thermoplastic hyperbranched polyurethanes. There were two strong diffraction peaks at $2\theta = 21.6$ and 23.7° due to

Table II. Thermal Properties and Degree of Crystallinity of the Hyperbranched Polyurethanes

Code	T_m (°C)	Degree of crystallinity (%)	T_{ON} (°C)	T_{MAX} (°C)	T_{END} (°C)
CHBPU	42.8	20.9	234	332	441
MHBPU	40.7	23.2	243	371	452
SHBPU	40.1	21.1	243	360	450
HBPU	39.4	21	243	346	443

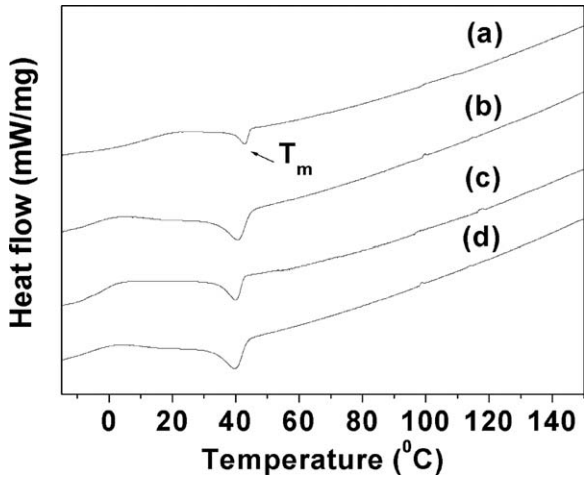

Figure 5. DSC curves for (a) CHBPU, (b) MHBPU, (c) SHBPU, and (d) HBPU.

the (100) and (200) planes of PCL crystals. *M. ferrea* L. seed-oil-based polyurethane showed the highest crystallinity compared to the other vegetable-oil-based polyurethanes.

NMR Study

The structure of the hyperbranched polyurethanes was studied by ^{1}H-NMR spectral analyses. ^{1}H-NMR spectra of all of the hyperbranched polyurethanes are shown in Figure 3. The ^{1}H-NMR spectrum of polyurethane confirmed the presence of the urethane group, TDI moieties, and other characteristic moieties, such as double bonds, chain —CH_2—, and terminal —CH_3. The peaks at $\partial = 0.80–0.87$, 1.19–1.27, and $\partial = 1.47–1.51$ ppm were due to the terminal methyl group, all internal —CH_2— groups, and the protons of the —CH_2— groups attached next to the terminal methyl group of the fatty acid chain of the MG of the oil, respectively.[23,26] The protons of allylic —CH_2—, —CH_2— adjacent to —O— of the urethane group and —CH_3 of TDI showed peaks at $\partial = 2.19–2.26$, 2.23–2.27, and 2.40–2.68 ppm, respectively. The —CH_2— protons of the triethanolamine moiety attached to the urethane linkages and —CH_2— protons attached to —OH groups were found at $\partial = 3.1–3.3$ and 3.96–4.03 ppm, respectively. The integration ratio of these two peaks indicated the extent of substitution of the —OH of the branch-generating moiety, triethanolamine. The observed ratio was found to be 2.50 for the CHBPU, which indicated that out of three —OH groups, 2.50 groups were substituted; that is, the degree of branching was about 0.83. Similarly, the degrees of branching were found to be 0.76, 0.70, and 0.64 for MHBPU, SHBPU, and HBPU, respectively. The protons of the aromatic moiety were observed around $\partial = 7.7–8.00$ ppm. However, there was another peak for the castor-oil-based hyperbranched polyurethane at $\partial = 3.8$ ppm for the —CH— proton attached to the —OH of the ricinoleic moiety. All of the previous spectral analyses confirmed the formation of the hyperbranched polyurethane. The structures and composition of all of the vegetable oils that we used are given in Table I.

Thermal Properties

The thermal stabilities of all of the hyperbranched polyurethanes are shown in Figure 4. The thermal stability of the polyurethane depended on the structures of the hard segment and soft segment, the degree of the urethane linkage, the hard segment to soft segment ratio, the extent of physical crosslinking, and the molecular weight and its distribution. From the results, we observed that the synthesized polyurethane exhibited a two-step degradation pattern. The first step was due to the degradation of the aliphatic chains and the breakage of the urethane linkages, whereas the second step was due to the degradation of the aromatic moieties. From the thermograms, we observed that the castor-oil-based polyurethane showed the lowest thermal stability. The hydroxyl functionality of the castor oil was higher than the other oils, and therefore, the degree of urethane linkage was greater. It was reported that higher the degree of urethane linkage is, the lower the thermal degradation will be.[27] The *M. ferrea* L. seed-oil-based polyurethane showed the highest thermal stability compared to the other different vegetable-oil-based polyurethanes. This may have been due to the higher crystallinity, as supported by the XRD study. The onset decomposition temperature (T_{ON}), temperature corresponding to the maximum rate of weight loss (T_{MAX}), and initiation of end-set decomposition temperature (T_{END}) for all of the hyperbranched polyurethanes are shown in Table II and in the thermograms (Figure 4).

DSC curves of all of the hyperbranched polyurethanes are shown in Figure 5. As shown in the figure, the castor-oil-based hyperbranched polyurethane showed the highest T_m (Table II). In the castor-oil-based polyurethane, the degree of urethane linkages was greater, and hence, the secondary interactions, such as H-bonding and polar–polar interactions, were also greater. The crystallinity of these hyperbranched polyurethanes came from the crystalline nature of the PCL moiety. The crystalline peak at about 40°C was due to the PCL moiety present in the

Table III. Mechanical Properties of the Hyperbranched Polyurethanes

Property	CHBPU	MHBPU	SHBPU	HBPU
Tensile strength (MPa)	7.5 ± 0.2	6.2 ± 0.2	5 ± 0.4	5.4 ± 0.3
Elongation at break (%)	607 ± 3.2	614 ± 3.4	620 ± 3.1	595 ± 3.3
Scratch hardness (kg)	6 ± 0.2	5.4 ± 0.1	5 ± 0.1	5 ± 0.2
Impact resistance (m)[a]	0.9 ± 0.05	0.9 ± 0.05	0.9 ± 0.05	0.9 ± 0.05
Bending (m)	<0.001	<0.001	<0.001	<0.001
Gloss (60°)	88 ± 3	86 ± 2	85 ± 3	85 ± 3

[a] 1.0 m was the limit of the instrument.

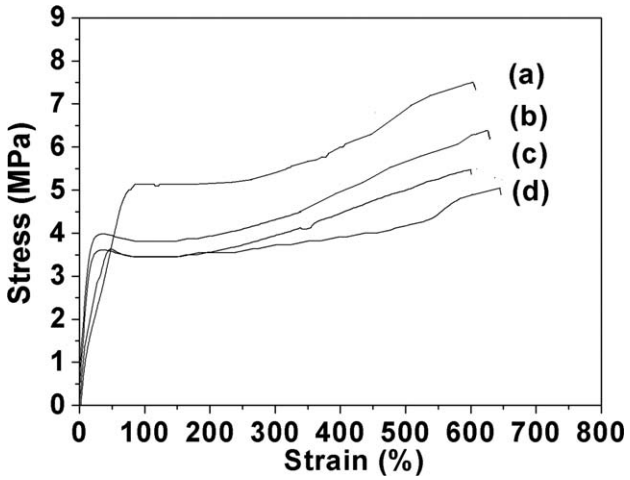

Figure 6. Stress–strain curves for (a) CHBPU, (b) MHBPU, (c) HBPU, and (d) SHBPU.

polymer chains, as supported by various studies from the literature.[28] No other T_m was found for this vegetable-oil-based polyurethane, as supported by earlier reports on similar polyurethanes.[29] The hyperbranched polymers as such were amorphous, but in this case, as a crystalline, long-segmented macroglycol, PCL was used, so a crystalline peak was observed in the DSC curves.

Mechanical Properties

The mechanical properties of all of the hyperbranched polyurethanes are shown in Table III, and the stress–strain profiles are shown in Figure 6. The performance of the polyurethane depends on the degree of the urethane groups, virtual or physical crosslinking density, and the various interactions, such as H bonding and polar–polar interactions. All of the polyurethanes showed overall good tensile strength. However, the castor-oil-based polyurethane showed the highest tensile strength. This may have been due to the unusual characterization of the castor oil, which is typically composed of 95% ricinoleic acid and has an average hydroxyl value of 2.7. Therefore, the degree of urethane linkages and physical crosslinking was higher in the castor-oil-based polyurethane than the others. However, the elongation at break was lower than the other vegetable-oil-based polyurethanes because of the rigidity of the structure that was generated through various secondary interactions in the polymer chains. All of the synthesized polyurethanes exhibited overall good scratch hardness. However, the castor-oil-based polyurethane exhibited the highest scratch hardness because of the increased overall toughness of the material. All of the synthesized vegetable-oil-based polyurethanes showed excellent impact resistance. The impact resistance of the material may have been due to the angle of toughness of the films, that is, the ability to absorb the applied external energy and the transfer of energy to its adjacent molecular networks. All of the samples exhibited good flexibility, as shown by the bending test, as the films could be bent onto a rod 1 mm in diameter without any fracture. This was due to the high flexibility of the soft segments and the presence of long-chain fatty acid moieties in the structure of the polyurethanes. The results revealed that the castor-oil-based polyurethane exhibited mechanical properties superior to those of the other vegetable-oil-based polyurethanes.

Shape-Memory Study

The shape-memory behaviors of the different hyperbranched polyurethanes are shown in Figure 7. The samples were

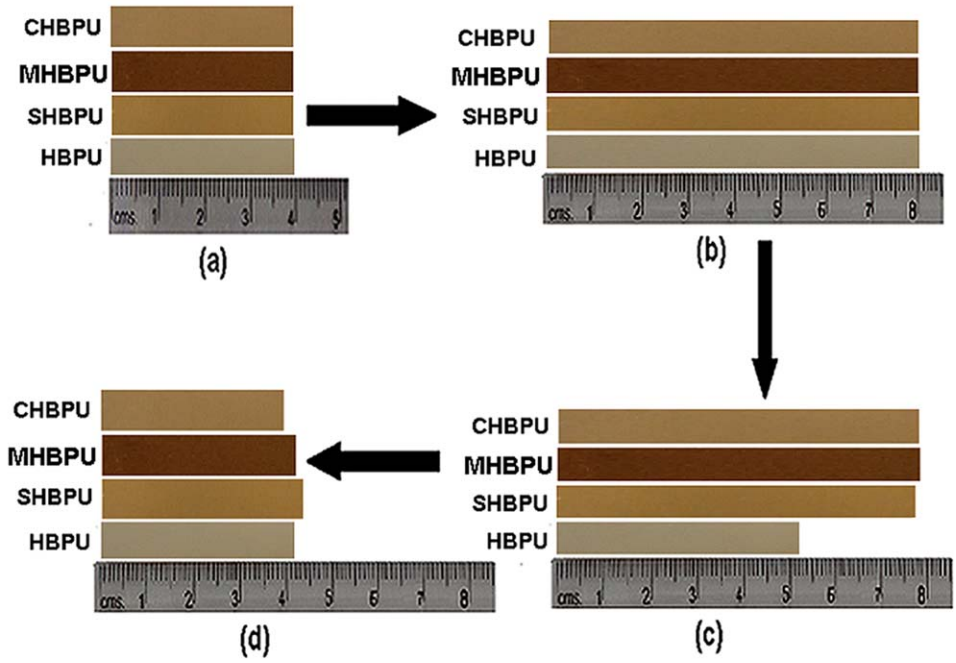

Figure 7. Shape-memory behaviors of the hyperbranched polyurethanes: (a) original shape, (b) extended shape, (c) fixed shape, and (d) recovered shape. [Color figure can be viewed in the online issue, which is available at wileyonlinelibrary.com.]

Table IV. Shape-Memory Behavior of the Hyperbranched Polyurethanes

Sample code	Shape fixity (%)	Shape recovery (%)
CHBPU	98± 0.1	98.5 ± 0.2
MHBPU	98 ± 0.2	96 ± 0.1
SHBPU	96.5 ± 0.3	94.8 ± 0.2
HBPU	32.5 ± 0.3	96.5 ± 0.1

stretched above T_m (60°C) of the hyperbranched polyurethanes and were subsequently frozen at a low temperature (0 to 5°C) to fix the deformed shape. The shape fixity temperature of 0–5°C was chosen on the basis of the fact that it could be achieved easily under the experimental conditions that we used and because it was a much lower temperature than the crystalline T_m of the soft segment. The crystalline T_m was considered the switching temperature because the melting transition was sharper than T_g. All of the vegetable-oil-based polyurethanes exhibited good shape fixity; this indicated that the micro-Brownian movements of the molecular chains in the physical network of the soft segment were frozen at the fixing temperature and, thereby, stored the applied load as strain energy. The vegetable-oil-based polyurethanes showed a higher shape fixity than the oil-free polyurethane. This may have been due to the presence of long-chain fatty acid moieties in the structure, which enhanced the secondary interactions during the vitrification. All of the vegetable-oil-based polyurethanes showed good shape recovery, although the castor-oil-based one showed the best shape recovery (Table IV). This could be attributed to the presence of more physical crosslinking due to the higher urethane linkages, which caused the storage of more deformed energy in the system. The sample immediately released the deformed stored energy and returned to its original shape on reheating. The *M. ferrea* L. seed-oil-based hyperbranched polyurethane also exhibited good shape recovery. This may have been due to the presence of various secondary interactions and the highly crystalline region of this hyperbranched polyurethane. No significant change in shape fixity or shape recovery was obtained for any of the hyperbranched polyurethanes for five cycles of testing.

CONCLUSIONS

In this study, different vegetable-oil-based polyurethanes were synthesized successfully. All of the synthesized polyurethanes showed overall good performance. However, the castor-oil-based hyperbranched polyurethane exhibited the highest tensile strength, whereas the *M. ferrea* L. seed-oil-based one showed the highest thermal stability among all of the studied hyperbranched polyurethanes. The castor-oil-based polyurethane showed the highest shape recovery, although all of the polyurethanes showed good shape fixity except the oil-free one. Thus, the characteristics of the oils had a strong influence on the performance and shape-memory effect of the hyperbranched polyurethanes. These synthesized vegetable-oil-based hyperbranched polyurethanes might be used in the different potential fields, such as in surgical sutures, catheters, drug delivery, microactuators, and sensors.

ACKNOWLEDGMENTS

The authors express their gratitude and thanks to the research project assistance granted by the Department of Science and Technology, India (contract grant number SR/S3/ME/0020/2009-SERC, July 9, 2010); Special Assistant Program (SAP) (University Grants Commission), India (contract grant number F.3-30/2009, System and Program Development (SAP)-II); and FIST-II (Fund for Improvement of Science and Technology Infrastructure in Higher Educational Institutions (FIST)-Phase two) phase two program 2009 (Department of Science and Technology), India (contract grant number SR/FST/CSI-203/209/1, May 6, 2010).

REFERENCES

1. Hu, J.; Meng, H.; Li, G.; Ibekwe, S. I. *Smart Mater. Struct.* **2012**, *21*, 053001.
2. Dong, J.; Weiss, R. *Macromolecules* **2011**, *44*, 8871.
3. Small, W.; Singhal, P.; Wilson, T. S.; Maitland, D. J. *J. Mater. Chem.* **2010**, *20*, 3356.
4. Yu, K.; Xie, T.; Leng, J.; Ding, Y.; Qi, H. *J. Soft Matter* **2012**, *8*, 5687.
5. Liu, C.; Qin, H.; Mather, P. T. *J. Mater. Chem.* **2007**, *17*, 1543.
6. Farzaneh, S.; Fitoussi, J.; Lucas, A.; Bocquet, M.; Tcharkhtchi, A. *J. Appl. Polym. Sci.* **2012**, 128, 3240.
7. Choi, N. Y.; Lendlein, A. *Soft Matter* **2007**, *3*, 901.
8. Lendlein, A.; Zotzmann, J.; Feng, Y.; Alteheld, A.; Kelch, S. *Biomacromolecules* **2009**, *10*, 975.
9. Jang, M. K.; Hartwig, A.; Kim, B. K. *J. Mater. Chem.* **2009**, *19*, 1166.
10. Min, C.; Cui, W.; Bei, J.; Wang, S. *Polym. Adv. Technol.* **2007**, *18*, 299.
11. Garle, A.; Kong, S.; Ojha, U.; Budhlall, B. M. *Appl. Mater. Interfaces* **2012**, *4*, 645.
12. Zini, E.; Scandola, M. *Biomacromolecules* **2007**, *8*, 3661.
13. Zhang, J.; Wu, G.; Huang, C.; Niu, Y.; Chen, C.; Chen, Z.; Yang, K.; Wang, Y. *J. Phys. Chem. C* **2012**, *116*, 5835.
14. Xue, L.; Dai, S.; Li, Z. *Macromolecules* **2009**, *42*, 964.
15. Xia, Y.; Larock, R. C. *Green Chem.* **2010**, *12*, 1893.
16. Sharma, V.; Kundu, P. P. *Prog. Polym. Sci.* **2008**, *33*, 1199.
17. Meier, M. A. R.; Metzger, J. O.; Schubert, U. S. *Chem. Soc. Rev.* **2007**, *36*, 1788.
18. Tan, S. G.; Chow, W. S. *Polym. Plast. Technol. Eng.* **2010**, *49*, 1581.
19. Sharma, V.; Kundu, P. P. *Prog. Polym. Sci.* **2006**, *31*, 983.
20. Zlatanic, A.; Lava, C.; Zhang, W.; Petrovic, Z. S. *J. Polym. Sci. Part B: Polym. Phys.* **2004**, *42*, 809.
21. Javni, I.; Petrovic, Z. S.; Guo, A.; Fuller, R. *J. Appl. Polym. Sci.* **2000**, *77*, 1723.
22. Karak, N.; Maiti, S. Dendrimers and Hyperbranched Polymers—Synthesis to Applications; MD Publication: New Delhi, **2008**.

23. Dutta, S.; Karak, N. *Polym. Int.* **2006**, *55*, 49.
24. Jung, H. C.; Kang, S. J.; Kim, W. N.; Lee, Y. B.; Choe, K. H.; Hong, S. H.; Kim, S. B. *J. Appl. Polym. Sci.* **2000**, *78*, 624.
25. Huang, J.; Zhang, L. *Polymer* **2002**, *43*, 2287.
26. Deka, H.; Karak, N. *Prog. Org. Coat* **2009**, *66*. 192.
27. Chattopadhyay, D. K.; Webster, D. C. *Prog. Polym. Sci.* **2009**, *34*, 1068.
28. Karak, N.; Rana, S.; Cho, J. W. *J. Appl. Polym. Sci.* **2009**, *112*, 736.
29. Deka, H.; Karak, N. *Nanoscale Res. Lett.* **2009**, *4*, 758.